Pergamon

Scripta Materialia, Vol. 37, No. 6, pp. 837-842, 1997
Elsevier Science Ltd

1359-6462/97 $17.00 + .00

PII S1359-6462(97)00187-5

A STUDY OF VACUUM CARBURIZATION OF AN EQUIATOMIC TiNi SHAPE MEMORY ALLOY

S.K. Wu and C.Y. Lee
Institute of Materials Science and Engineering, National Taiwan University
Taipei, Taiwan 106, ROC

H.C. Lin
Department of Materials Science, Feng Chia University
Taichung, Taiwan 400, ROC

(Received February 10, 1997)
(Accepted April 27, 1997)

Introduction

TiNi alloys are known as the most important shape memory alloys (SMAs) because they exhibit thermoelastic martensitic transformation. They are known for their many applications which are based on shape memory effect (SME) [1] and pseudoelasticity (PE) [2,3]. This stems from the fact that TiNi alloys have superior properties in ductility, biocompatibility and recoverable strain. Recently, TiNi alloys have been observed to exhibit an excellent wear resistance [4-6], which is an important property in some biomedical applications, such as medical guide-wires, artificial bone-joints, etc. In fact, the B2 phase (austenite parent phase) of TiNi alloys can really exhibit an excellent wear resistance due to their rapid hardening and pseudoelastic property [7]. But the wear resistance of the B19′ martensite phase of TiNi alloys is still too weak and needs to be improved for some applications. It is well known that surface coating of titanium carbides (TiC) is commonly used to improve the fatigue and wear resistance of metals and alloys. However, to our knowledge, there have been few investigations on the surface coating of TiNi alloys with titanium carbides [8,9]. The main obstacle for TiC coating is the high affinity of titanium to oxygen [10]. This problem is overcome in the present study by the use of vacuum carburization due to the rare content of oxygen in the carburizing atmosphere. The surface hardness and wear characteristics of the carburized equiatomic TiNi alloy are studied. The effects of TiC film on the transformation temperatures and shape memory ability are also discussed in this paper.

Experimental Details

A conventional tungsten arc melting technique was employed to prepare the equiatomic TiNi alloy. Titanium (purity, 99.7%) and nickel (purity, 99.9%), amounting to 100g, were melted and remelted at least six times in an argon atmosphere. The as-melted buttons were homogenized at 1000°C in a vacuum furnace for 3 days and then hot-rolled at 850°C to a plate of 1.5 mm thickness. Specimens with

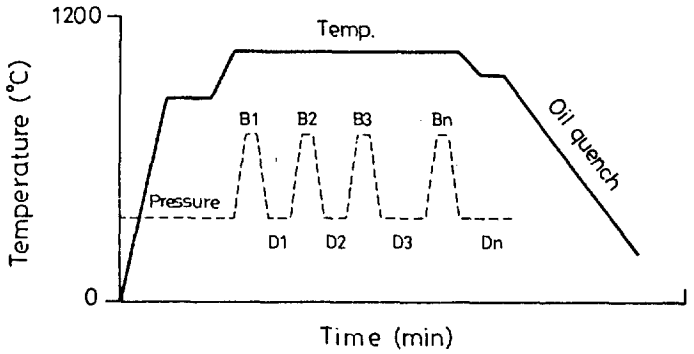

Figure 1. Schematic diagram of vacuum-carburizing process.

dimensions of 10 mm × 30 mm × 1.5 mm were then cut from the plate using a low speed diamond saw. The specimen surface was then polished with 2000 grit emery paper. Before carburizing, all specimens were cleaned ultrasonically in acetone to remove surface grease. Vacuum carburization was carried out in a furnace model FOURS B.M.I. made in France. The carburizing process is illustrated in Fig. 1. In Fig. 1, the vacuum pressure during carburizing (B_1 ~ Bn) is 0.7 bar and the quenching pressure (D_1 ~ Dn) is 0.5 bar. Bn and Dn indicate the nth carburizing process. The flow rate of carburing gas C_3H_8 was 40 liters per hour. The carburing temperatures were selected as 930°C and 980°C.

The microstructures of the carburized layers were studied by X-ray diffraction (XRD), using a Philips PW1710 XRD with Cu Kα radiation. The power was 40 kV × 30 mA and the 2θ scanning rate was 3°min^{-1}. The concentration profiles of Ti, Ni and C in the carburized layers of $Ti_{50}Ni_{50}$ specimens were analyzed using a JEOL JXA-8600SX electron probe microanalyzer (EPMA) with a probe size 1μm. In order to obtain a precise composition analysis, the surface of the mounted specimens were carefully polished without any etching. The surface hardness was tested with a microvickers tester with a load of 100 gf for 15 seconds. For each specimen, at least five different locations were tested. The DSC measurement was conducted to measure the martensitic transformation temperatures. A DuPont 2000 thermal analyzer equipped with a quantitative scanning system 910 DSC cell and a cooling accessory LNCA II was used. Measurements were carried out at a controlled cooling/heating rate of 10°C min^{-1}. Heats of transformation (ΔH) were automatically calculated from the areas under DSC peaks by means of an equipment software package. The wear tests were performed using a TE-53 type uni-directional sliding wear machine made by Plint & Partners Co. in England. The JIS SKS-95 steel, with hardness Hv = 700, was used as the wear-resistant material. The tests were conducted at a constant wear load of 10 N and sliding speed of 62.8 cm s^{-1}. The friction coefficient was automatically calculated by a digit computer during the sliding wear process. The shape memory effect (SME) was examined by a bending test [11]. The surface bending strain, ε_s, was 8% and the shape recovery, R_{SME}, was measured after a complete reverse martensitic transformation.

Results and Discussion

A. Microstructure and Composition Analysis of Vacuum-Carburized $Ti_{50}Ni_{50}$ Alloy

After vacuum carburizing, the $Ti_{50}Ni_{50}$ specimens show a homogeneous surface morphology. Fig. 2(a,b) show the XRD patterns of $Ti_{50}Ni_{50}$ specimens after vacuum carburizing at 930°C × 4 times, and

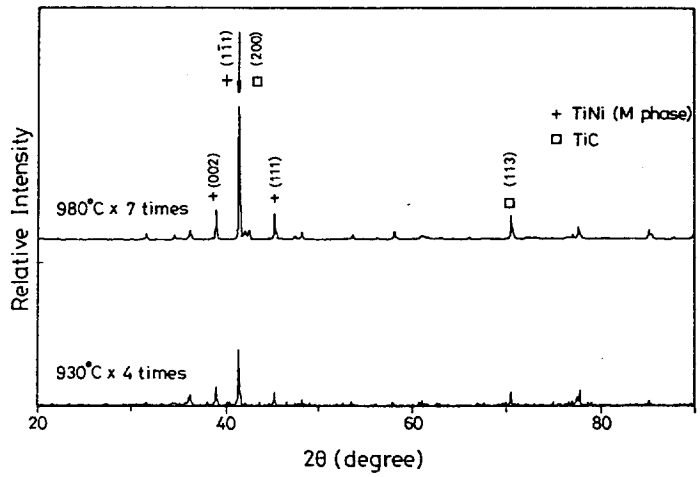

Figure 2. XRD patterns of $Ti_{50}Ni_{50}$ specimens with vacuum carburizing. (a) 930°C × 4 times and (b) 980°C × 7 times.

980°C × 7 times, respectively. As shown in Fig. 2(a,b), in addition to the peaks of TiNi B19′ martensite, a strong peak of the TiC phase appears in the XRD patterns. The intensity of the TiC peak increases with increasing carburizing temperature and carburizing time. This indicates that the thickness of the TiC layer increases with increasing carburizing temperature and time. Fig. 3 shows the EPMA line scan of a $Ti_{50}Ni_{50}$ specimen carburized at 980°C for 7 times. The intensity of the C Kα line increases from the surface to a maximum in the carburized layer. It then decreases continuously and levels off in the TiNi matrix. It is difficult to confirm the existence of a carbon diffusion layer from Fig. 3 because of the weak concentration of carbon in the TiNi matrix. The intensity of the Ti Kα line also increases from the surface to a maximum at the carburized layer/TiNi matrix interface, and then gradually decreases and levels off in the TiNi matrix. The intensity of the Ni Kα line continuously increases in the carburized layer and then levels off in the TiNi matrix. From the results of XRD in Fig. 2 and the variations of Ti, Ni and C concentrations in Fig. 3, we have confirmed that a TiC film forms

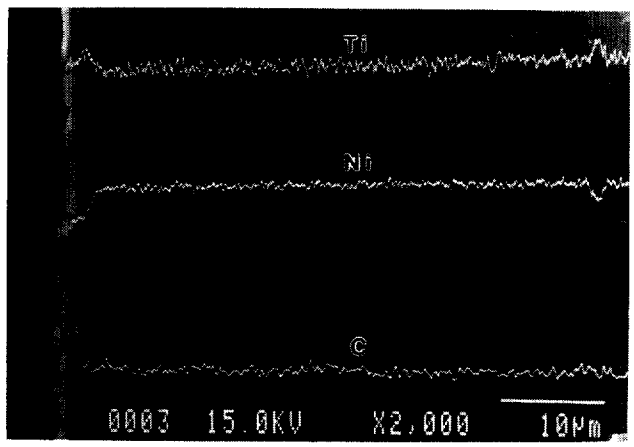

Figure 3. EPMA line scan of the 980°C × 7 times carburized $Ti_{50}Ni_{50}$ specimen.

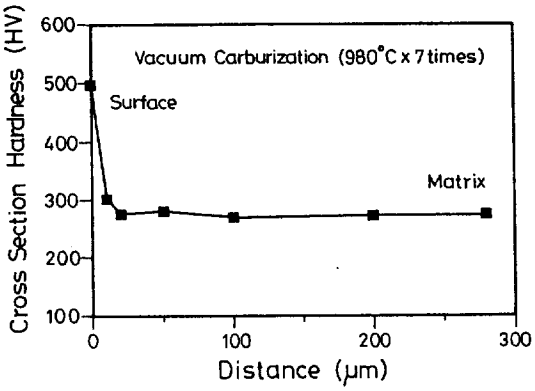

Figure 4. The cross-sectional hardness vs. distance from the surface for the carburized $Ti_{50}Ni_{50}$ specimen.

in the surface of vacuum-carburized $Ti_{50}Ni_{50}$ specimens. In Fig. 3, the thickness of TiC film is about 2 μm. From Fig. 3, one can find that the TiC film can dissolve quite a number of nickel atoms.

B. Effects of Vacuum Carburization on the Surface Hardness and Wear Characteristics of the $Ti_{50}Ni_{50}$ Alloy

Fig. 4 shows the cross-sectional hardness vs. distance from the surface for the carburized $Ti_{50}Ni_{50}$ specimen. Because the reported hardness of the TiC phase (Knoop hardness HK = 2470) [12] is so much higher than that of $Ti_{50}Ni_{50}$ martensite (Hv = 270), the surface hardness of the carburized $Ti_{50}Ni_{50}$ specimen is increased, as shown in Fig. 4. However, the maximum surface hardness can not exhibit an expected high value, say, only 500Hv in Fig. 4. This phenomenon comes from the fact that the TiC film is so thin and hence the indentation of the hardness measurement will reach the soft TiNi martensite. This feature causes the average hardness of the carburized surface to not be as high as the TiC phase.

Fig. 5 shows the friction coefficients of the $Ti_{50}Ni_{50}$ specimens with and without vacuum carburization at 980°C for 7 times. As shown in Fig. 5, the friction coefficients of the carburized specimen are lower than those of the non-carburized specimen. This result comes from the fact that the wear interfaces are TiC layer and SKS-95 steel, and hence friction coefficients maintain low values due to their high hardness. This indicates that the wear characteristics of $Ti_{50}Ni_{50}$ specimens can be effectively improved by vacuum carburization.

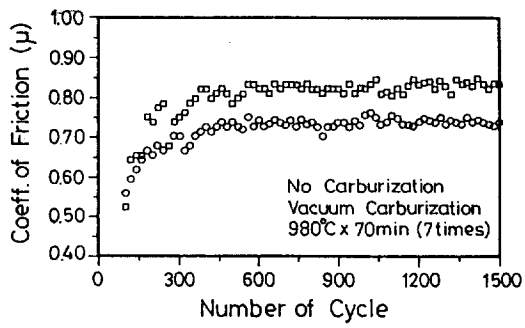

Figure 5. The friction coefficients of $Ti_{50}Ni_{50}$ specimens with and without vacuum carburization at 980°C for 7 times.

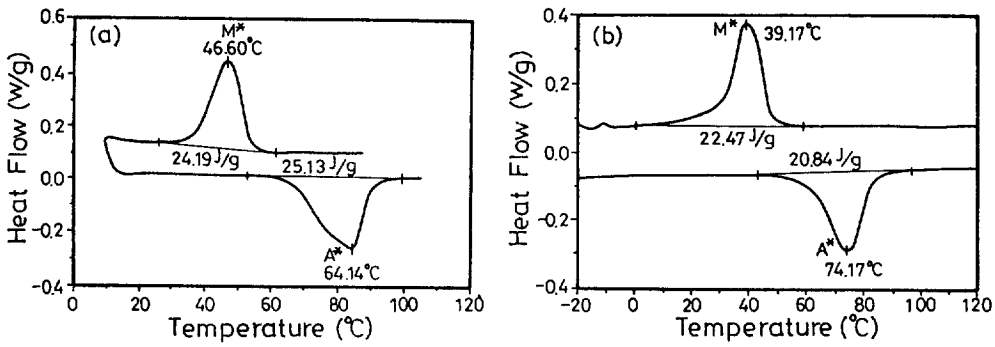

Figure 6. The DSC curves of $Ti_{50}Ni_{50}$ specimens. (a) without vacuum carburization and (b) with vacuum carburization at 980°C for 7 times.

C. Effects of Vacuum Carburization on the Transformation Temperatures and Shape Memory Ability of the $Ti_{50}Ni_{50}$ Alloy

Fig. 6(a-b) show the DSC curves of $Ti_{50}Ni_{50}$ specimens with and without vacuum carburization at 980°C for 7 times, respectively. Fig. 6 (a) represents a typical DSC curve of stress-free $Ti_{50}Ni_{50}$ alloy in which the exothermic and endothermic peaks are associated with the martensitic transformation of B2 ↔ B19′. The DSC curves for the carburized specimen, as shown in Fig. 6(b), exhibit similiar martensitic transformation behaviors. However, the transformation temperatures are shifted towards lower ones. This phenomenon may be ascribed to two factors. First, the constrained stress originating from the TiC layer will depress the martensitic transformation. Second, the penetration of C atoms or other impurities into the TiNi matrix during the vacuum carburizing process will also depress the transformation temperatures [13].

Table 1 presents the measured shape recovery, R_{SME}, after a complete reverse martensitic transformation (by heating to 300°C) for the vacuum-carburized $Ti_{50}Ni_{50}$ alloy. From Table 1, the shape recovery is found to be slightly reduced due to the carburization. This result is reasonable because the TiC phases do not exhibit a shape memory effect. Furthermore, their constrained effect on the TiNi matrix will also depress the shape recovery of the TiNi matrix.

Summary

The vacuum-carburized $Ti_{50}Ni_{50}$ alloy consists of a TiC layer in the outer surface, the thickness of which increases with increasing carburizing temperature and time. The carburized TiNi specimens, being hardened by the TiC phase, show improved wear characteristic. The martensitic transformation

TABLE 1
The Measured Shape Recovery, R_{SME}, After Complete Reverse Martensitic Transformation for the Vacuum-Carburized Equiatomic TiNi Alloys

specimen's condition	bending angle at martensite phase (degree)	measured angle after heated at 300°C (degree)	R_{SME} (%)
no carburized	74	7	90.5
carburized at 980°C × 7 time	55	13	76.4

temperatures are depressed slightly to lower ones due to the constraint stress originating from the TiC layer, and the penetration of C atoms or other impurities into the TiNi matrix during the carburizing process. At the same time, the shape recovery of the carburized TiNi alloy is also slightly reduced because the TiC phase does not exhibit a shape memory effect and its constraint effect will also depress the shape recovery of the TiNi matrix.

Acknowledgement

The authors are pleased to acknowledge the financial support of this research by the National Science Council (NSC), Republic of China, under Grant NSC 84-2216-E002-027.

References

1. S. Miyazaki, K. Otsuka and Y. Suzuki, Scripta Metall., 15 (1981) 287-292.
2. S. Miyazaki, Y. Ohmi, K. Otsuka and Y. Suzuki, ICOMAT-82, J. Phys., 43 (1982) C4-255-260.
3. S. Miyazaki, T. Imai, Y. Igo and K. Otsuka, Metall. Trans. A, 17A (1986) 115-120.
4. J.L. Jin and H.L. Wang, Acta Metall. Sinica, 24 (1988) A66-69.
5. D.Y. Li, Scripta Metall., 34 (1996) 195-200.
6. P. Clayton, Wear 162-164 (1993) 202-210.
7. H.M. Liao, H.C. Lin, J.L. He, K.C. Chen and K.M. Lin, Proc. International Conference on Displacive Transformations, 1996, in press.
8. S. Lesokhin and L. Levin, "Design fundamentals of High Temperature Composites, Intermetallics, and Metal-Ceramics Systems", ed. by R.Y. Lin, Y.A. Chang, R.G. Reddy and C.T. Liu ,TMS, 1995, pp. 399-411.
9. A. Hedayat, J. Rechtien and K. Mukherjee, Journal of Materials Science: Materials in Medicine, 3 (1992) 65-74.
10. K.S. Edmund, The Refractory Carbides, New York, Academic Press, 1967.
11. H.C. Lin and S.K. Wu, Scripta Metall. Mater., 26 (1992) 59-62.
12. *Handbook of Chemistry and Physics*, CRC Press, Florida, USA, 58th ed., 1978, pp. F-24.
13. T. Honma, *Shape Memory Alloys*, Gordon and Breach Science Publishers, Amsterdam, 1987, pp. 89-101.